Computer Methods in Applied Mechanics and Engineering 95 (1992) 221–242
North-Holland

Incompressible flow computations with stabilized bilinear and linear equal-order-interpolation velocity-pressure elements*

T.E. Tezduyar, S. Mittal, S.E. Ray and R. Shih

Department of Aerospace Engineering, Army High-Performance Computing Research Center, and Mechanics and Minnesota Supercomputer Institute, University of Minnesota, 1200 Washington Avenue South, Minneapolis, MN 55415, USA

Received 18 September 1990

Finite element formulations based on stabilized bilinear and linear equal-order-interpolation velocity-pressure elements are presented for computation of steady and unsteady incompressible flows. The stabilization procedure involves a slightly modified Galerkin/least-squares formulation of the steady-state equations. The pressure field is interpolated by continuous functions for both the quadrilateral and triangular elements used. These elements are employed in conjunction with the one-step and multi-step time integration of the Navier–Stokes equations. The three test cases chosen for the performance evaluation of these formulations are the standing vortex problem, the lid-driven cavity flow at Reynolds number 400, and flow past a cylinder at Reynolds number 100.

1. Introduction

In finite element computation of incompressible flows there are two main sources of potential numerical instabilities associated with the Galerkin formulation of a problem. One is due to the presence of advection terms and can result in spurious node-to-node oscillations primarily in the velocity field. Such oscillations become more significant for high Reynolds number flows and flows with sharp layers in the solution. The other source of instability is produced if an inappropriate combination of interpolation functions for the velocity and pressure is used. These instabilities usually appear as oscillations primarily in the pressure field.

We present certain stabilized finite element formulations using equal-order-interpolation velocity-pressure elements for the computation of steady and unsteady incompressible flows. The elements considered (see Fig. 1) are Q1Q1 (continuous bilinear velocity and pressure) and P1P1 (continuous linear velocity and pressure).

The stabilization is achieved by adding two terms to the standard Galerkin formulation of the problem. The first term, which, by itself, would lead to a formulation popularly known as the SUPG (streamline-upwind/Petrov–Galerkin) formulation, has been successfully used, as early as nearly a decade ago, for both incompressible and compressible flow problems [1, 2]. It prevents, without introducing excessive numerical dissipation, the oscillations caused by the presence of advection terms. In applications to incompressible flows at finite Reynolds numbers, generally, elements with bilinear velocity and constant pressure were used [1]. It was pointed out in [3] that one-step time integration of the semi-discrete equations, obtained by

* This research was sponsored by NASA-Johnson Space Center under grant NAG 9-449, and by NSF under grant MSM-8796352.

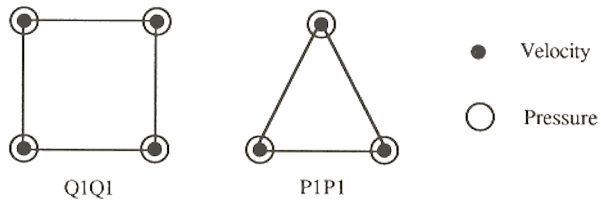

Fig. 1. The velocity-pressure elements used

using such elements, results in solutions which appear to involve more numerical diffusion than one would like to have. The multi-step T6 formulation introduced in [3], on the other hand, was shown to lead to solutions involving much less numerical diffusion. The SUPG method has also been successfully applied to the vorticity-stream function formulation of the time-dependent incompressible flows, including those with multiply-connected domains [4].

The second stabilizing term is a generalization, to finite Reynolds number flows, of the Petrov–Galerkin term proposed for Stokes flows [5]. Instead of using unequal-order interpolation functions for the velocity and pressure (see for example [6]), with this stabilizing term one can use equal-order functions without generating oscillations in the pressure field. We will refer to this term as the PSPG (pressure-stabilizing/Petrov–Galerkin) term. In the zero Reynolds number limit this term reduces to the one proposed in [5].

The Galerkin/least-squares formulation, which appears to be a more systematic and general approach to the stabilization of flow computations, has been shown to be robust and accurate when applied to compressible flows [7, 8] and Stokes flows [9]. In this paper we obtain the SUPG and PSPG stabilizing terms, for time-dependent incompressible flows with finite Reynolds numbers, by considering the Galerkin/least-squares formulation of the steady-state equations. The stabilizing terms are obtained by minimizing the sum of the squared residual of the momentum equation integrated over each element domain. This procedure leads to a least-squares term with contributions from the advective, pressure and the viscous stress terms. These least-squares terms are added, with a certain weighting factor, to the Galerkin formulation of the problem. At the element interiors the contribution to the weighting function from the viscous term is identically zero for the P1P1 element and is neglected for the Q1Q1 element. The contributions from the advective and pressure terms give the SUPG and PSPG stabilizers, respectively. In the present formulation the weighting factors for the SUPG and PSPG terms slightly differ from each other.

We have incorporated these stabilizing terms within both the one-step and the multi-step (T6) time integration of the equations. The T6 formulation [3] is an extension of the T3 formulation [3]. The T3 formulation is a three-step method and starts out with an operator splitting scheme in which the pressure and the viscous terms are treated implicitly in the first and third steps, while the advective terms are treated implicitly in the second step. This type of splitting is a special case of the θ-scheme presented in [10]. In the T6 formulation, each step of the T3 formulation is subdivided into two sub-steps to isolate the advective terms, and the SUPG term is applied only to the sub-steps involving the advective terms. The PSPG term, on the other hand, is applied only to the sub-steps involving the pressure. The preliminary formulations involving the PSPG term with the T6 integration were given in [11].

We consider three numerical tests: the standing vortex problem [12], the lid-driven cavity flow at $Re = 400$, and flow past a circular cylinder at $Re = 100$. The standing vortex problem is used for determining the level of numerical dissipation involved. The lid-driven cavity problem involves singularities in the pressure field and, therefore, is regarded as a stringent test case. The cylinder problem has been studied by several researchers in the past and has become a benchmark problem (see for example [3, 6, 13]).

2. The incompressible Navier–Stokes equations

Let Ω and $(0, T)$ be the spatial and temporal domains, and let $x \in \bar{\Omega}$ and $t \in [0, T]$ represent the associated coordinates, where a superposed bar denotes the set closure. We consider the following velocity-pressure formulation of the Navier–Stokes equations for unsteady incompressible flows:

$$\rho\left(\frac{\partial u}{\partial t} + u \cdot \nabla u\right) - \nabla \cdot \sigma = 0\,, \quad \text{on } \Omega \times (0, T)$$

$$\nabla \cdot u = 0\,, \quad \text{on } \Omega \times (0, T)$$

where ρ and u are the density and velocity, and σ is the stress tensor given as

$$\sigma = -pI + 2\mu\varepsilon(u)$$

with

$$\varepsilon(u) = \tfrac{1}{2}(\nabla u + (\nabla u)^t)$$

Here p and μ represent the pressure and the dynamic viscosity, while I denotes the identity tensor. It is assumed that both Dirichlet and Neumann type boundary conditions could be imposed at different segments of the boundary Γ:

$$u = g\,, \quad \text{on } \Gamma_g\,,$$

$$n \cdot \sigma = h\,, \quad \text{on } \Gamma_h\,, \tag{6}$$

where Γ_g and Γ_h are complementary subsets of Γ.

3. The spatial and temporal discretizations

Let $\mathscr{E}$ denote the set of elements resulting from the finite element discretization of the computational domain Ω into subdomains Ω^e, $e = 1, 2, \ldots, n_{el}$, where n_{el} is the number of elements. We associate with $\mathscr{E}$ the finite dimensional space H^{1h} defined as

$$H^{1h} \quad \{\phi^h \mid \phi^h \in C^0(\bar{\Omega}),\ \phi^h|_{\Omega^e} \in P^1,\ \forall \Omega^e \in \mathscr{E}\}\,,$$

with P^1 representing the first-order polynomials. The trial and test function spaces are defined as

$$S_u^h = \{u^h \mid u^h \in (H^{1h})^{n_{sd}},\ u^h = g^h \quad \text{on } \Gamma_g\}\,, \tag{8}$$

$$V_u^h = \{w^h \quad \text{on } \Gamma_g\}\,, \tag{9}$$

$$S_p^h = V_p^h = \{q \quad q \in H^{1h}\}\,,$$

where n_{sd} is the number of space dimensions.

We write the stabilized Galerkin formulation of (1), (2) as follows: find $u^h \in S_u^h$ and $p^h \in S_p^h$ such that

$$\int_\Omega \boldsymbol{w}^h \cdot \rho\left(\frac{\partial \boldsymbol{u}^h}{\partial t} + \boldsymbol{u}^h \cdot \nabla \boldsymbol{u}^h\right) \mathrm{d}\Omega + \int_\Omega \varepsilon(\boldsymbol{w}^h) : \sigma^h \, \mathrm{d}\Omega$$
$$+ \sum_{e=1}^{n_{\mathrm{el}}} \int_{\Omega^e} \delta^h \cdot \left[\rho\left(\frac{\partial \boldsymbol{u}^h}{\partial t} + \boldsymbol{u}^h \cdot \nabla \boldsymbol{u}^h\right) - \nabla \cdot \sigma^h\right] \mathrm{d}\Omega$$
$$+ \sum_{e=1}^{n_{\mathrm{el}}} \int_{\Omega^e} \epsilon^h \cdot \left[\rho\left(\frac{\partial \boldsymbol{u}^h}{\partial t} + \boldsymbol{u}^h \cdot \nabla \boldsymbol{u}^h\right) - \nabla \cdot \sigma^h\right] \mathrm{d}\Omega$$
$$+ \int_\Omega q^h \rho \nabla \cdot \boldsymbol{u}^h \, \mathrm{d}\Omega = \int_{\Gamma_h} \boldsymbol{w}^h \cdot \boldsymbol{h}^h \, \mathrm{d}\Gamma \quad \forall \boldsymbol{w}^h \in V_{\boldsymbol{u}}^h \quad \forall q^h \in V_p^h$$

As can be seen from (11), two stabilizing terms are added to the standard Galerkin formulation of (1), (2); the one with δ^h is the SUPG (streamline-upwind/Petrov–Galerkin) term, and the one with ϵ^h is the PSPG (pressure-stabilizing/Petrov–Galerkin) term. The Petrov–Galerkin functions δ^h and ϵ^h are defined as

$$\delta^h = \tau_{\mathrm{SUPG}}(\boldsymbol{u}^h \cdot \nabla)\boldsymbol{w}^h \tag{12}$$

$$\epsilon^h = \tau_{\mathrm{PSPG}} \frac{1}{\rho} \nabla q^h , \tag{13}$$

where

$$\tau_{\mathrm{SUPG}} = \frac{h}{2\|\boldsymbol{u}^h\|} z(\mathrm{Re}_u) ,$$

$$\tau_{\mathrm{PSPG}} = \frac{h^\#}{2\|\boldsymbol{U}\|} z(\mathrm{Re}_U^\#$$

Here Re_u and $\mathrm{Re}_U^\#$ are the element Reynolds numbers which are based on the local velocity $\boldsymbol{u}^h$ and a global scaling velocity $\boldsymbol{U}$, respectively. That is,

$$\mathrm{Re}_u = \frac{\|\boldsymbol{u}^h\| h}{2\nu} ,$$

$$\mathrm{Re}_U^\# = \frac{\|\boldsymbol{U}\| h^\#}{2\nu}$$

where ν is the kinematic viscosity. The 'element length' h is computed by using the expression

$$h = 2\left(\sum_{a=1}^{n_{\mathrm{en}}} |\boldsymbol{s} \cdot \nabla N_a|\right)$$

where N_a is the basis function associated with node a, n_{en} is the number of nodes in the element, and $\boldsymbol{s}$ is the unit vector in the direction of the local velocity. The 'element length' $h^\#$, on the other hand, is defined to be equal to the diameter of the circle which is area-equivalent to the element. The function $z(\mathrm{Re})$ used in (14) and (15) is defined as

$$z(\mathrm{Re}) = \begin{cases} \mathrm{Re}/3 , & 0 \leqslant \mathrm{Re} \leqslant 3 \\ 1 , & 3 \leqslant \mathrm{Re} . \end{cases}$$

We have also experimented with an alternative (common) definition for τ_{SUPG} and τ_{PSPG}

$$\tau_{\mathrm{SUPG}} = \tau_{\mathrm{PSPG}} = \left[\left(\frac{2}{\Delta t}\right)^2 + \left(\frac{2\|\boldsymbol{u}^h\|}{h^{\#}}\right)^2 + 9\left(\frac{4\nu}{(h^{\#})^2}\right)^2\right]^{-1/2}$$

This expression is based on the one given in [8] for compressible flows. Equation (20) can also be written as

$$\tau_{\mathrm{SUPG}} = \tau_{\mathrm{PSPG}} = \frac{h^{\#}}{\cdot\cdot 1}\left[\left(\frac{1}{C_{\Delta t}}\right)^2 + 1 + \left(\frac{3}{\mathrm{Re}^{\#}}\right)^2\right]^{-1/2}$$

where $C_{\Delta t}$ and $\mathrm{Re}_u^{\#}$ are the element Courant and Reynolds numbers, respectively, and are defined as

$$C_{\Delta t} = \frac{\|\boldsymbol{u}^h\|\,\Delta t}{h^{\#}}$$

$$\mathrm{Re}_u^{\#} = \frac{\|\boldsymbol{u}^h\| h^{\#}}{2\nu}$$

REMARK 1. For steady-state computations the $(1/C_{\Delta t})^2$ term is dropped. Notice that in this case, the limits of the expression given by (21), for Reynolds numbers zero and infinity, are very close to the limits of τ_{SUPG} and τ_{PSPG} given by (14) and (15).

REMARK 2. For very small Courant numbers the expression given by (21) reduces to $\frac{1}{2}\Delta t$, which means that the stabilizing term vanishes as the time step goes to zero.

The spatial discretization of (11) leads to the following set of non-linear ordinary differential equations:

$$(\boldsymbol{M} + \boldsymbol{M}_\delta)\boldsymbol{a} + \boldsymbol{N}(\boldsymbol{v}) + \boldsymbol{N}_\delta(\boldsymbol{v}) + (\boldsymbol{K} + \boldsymbol{K}_\delta)\boldsymbol{v} - (\boldsymbol{G} + \boldsymbol{G}_\delta)\boldsymbol{p} = \boldsymbol{F} + \boldsymbol{F}_\delta$$

$$\boldsymbol{G}^{\mathrm{t}}\boldsymbol{v} + \boldsymbol{M}_\epsilon\boldsymbol{a} + \quad \boldsymbol{N}_\epsilon(\boldsymbol{v}) + \quad \boldsymbol{K}_\epsilon\boldsymbol{v} + \quad \boldsymbol{G}_\epsilon\boldsymbol{p} = \boldsymbol{E} + \boldsymbol{E}_\epsilon\,,$$

where $\boldsymbol{v}$ is the vector of unknown nodal values of $\boldsymbol{u}^h$, $\boldsymbol{a}$ is the time derivative of $\boldsymbol{v}$, and $\boldsymbol{p}$ is the vector of nodal values of p^h. The matrices $\boldsymbol{M}$, $\boldsymbol{N}$, $\boldsymbol{K}$ and $\boldsymbol{G}$ are derived from the time-dependent, advective, viscous and pressure terms, respectively. The vector $\boldsymbol{F}$ is due to the Dirichlet and Neumann type boundary conditions (i.e., the $\mathbf{g}$ and $\mathbf{h}$ terms in (5) and (6)), whereas the vector $\boldsymbol{E}$ is due to the Dirichlet type boundary condition. The subscripts δ and ϵ identify the SUPG and PSPG contributions, respectively.

We first consider the temporal discretization of (24) and (25) by a one-step generalized trapezoidal rule; i.e., given $\boldsymbol{u}_n^h \in (S_u^h)_n$ find $\boldsymbol{u}_{n+1}^h \in (S_u^h)_{n+1}$ and $p_{n+1}^h \in S_p^h$ (we will refer to this as the T1 formulation). When written in an incremental form, the T1 formulation leads to

$$\boldsymbol{M}^*\,\Delta\boldsymbol{a} - \boldsymbol{G}^*\,\Delta\boldsymbol{p} = \boldsymbol{R}$$

$$(\boldsymbol{G}^{\mathrm{t}})^*\,\Delta\boldsymbol{a} + \boldsymbol{G}_\epsilon\,\Delta\boldsymbol{p} = \boldsymbol{Q}\,,$$

where

$$\boldsymbol{R} = \boldsymbol{F} + \boldsymbol{F}_\delta - [(\boldsymbol{M} + \boldsymbol{M}_\delta)\boldsymbol{a} + \boldsymbol{N}(\boldsymbol{v}) + \boldsymbol{N}_\delta(\boldsymbol{v}) + (\boldsymbol{K} + \boldsymbol{K}_\delta)\boldsymbol{v} - (\boldsymbol{G} + \boldsymbol{G}_\delta)\boldsymbol{p}]\,,$$

$$\boldsymbol{Q} = \boldsymbol{E} + \boldsymbol{E}_\epsilon - [\boldsymbol{G}^{\mathrm{t}}\boldsymbol{v} + \boldsymbol{M}_\epsilon \boldsymbol{a} + \boldsymbol{N}_\epsilon(\boldsymbol{v}) + \boldsymbol{K}_\epsilon \boldsymbol{v} + \boldsymbol{G}_\epsilon \boldsymbol{p}] ,$$

$$M^* = M + M_\delta + \alpha\, \Delta t\left(\frac{\partial N}{\partial \boldsymbol{v}} + \frac{\partial N_\delta}{\partial \boldsymbol{v}} + K + K_\delta\right)$$

$$\boldsymbol{G}^* = \boldsymbol{G} + \boldsymbol{G}_\delta ,$$

$$(G^{\mathrm{t}})^* = M_\epsilon + \alpha\, \Delta t\left(\frac{\partial N_\epsilon}{\partial \boldsymbol{v}} + K_\epsilon + G^{\mathrm{t}}\right)$$

The parameter α controls the stability and accuracy of the time integration algorithm.

REMARK 3. The equation systems (24) and (25) can be solved by treating the velocity explicitly in the momentum equation. Since the SUPG and PSPG supplements are applied to all terms in the momentum equation, in explicit computations the coefficient matrix of the pressure equation is generally not symmetric. All explicit T1 computations presented in this paper are based on a symmetrized coefficient matrix of the pressure equation, and the results are obtained with 2 passes per time step. In such computations $\boldsymbol{M}^*$, $\boldsymbol{G}^*$ and $(\boldsymbol{G}^{\mathrm{t}})^*$ are replaced with

$$\boldsymbol{M}^* = \boldsymbol{M}_{\mathrm{L}} ,$$

$$\boldsymbol{G}^* = \boldsymbol{G} ,$$

$$(\boldsymbol{G}^{\mathrm{t}})^* = \alpha\, \Delta t\, \mathbf{G}^{\mathrm{t}}$$

where $\boldsymbol{M}_{\mathrm{L}}$ is the lumped version of $\boldsymbol{M}$.
Next we summarize the T6 formulation [3].

(1 Find $\tilde{\boldsymbol{u}}^h_{n+\theta} \in (S^h_u)_{n+\theta}$ such that

$$\int_\Omega w^h \cdot \rho[(\tilde{u}^h_{n+\theta} - \boldsymbol{u}^h_n)/(\theta\, \Delta t) + \boldsymbol{u}^h_n \cdot \nabla \boldsymbol{u}^h_n]\, \mathrm{d}\Omega$$

$$+ \sum_{e=1}^{n_{\mathrm{el}}} \int_{\Omega^e} \delta^h \cdot [\rho((\tilde{\boldsymbol{u}}^h_{n+\theta} - \boldsymbol{u}^h_n)/(\theta\, \Delta t) + \boldsymbol{u}^h_n \cdot \nabla \boldsymbol{u}^h_n)]\, \mathrm{d}\Omega = 0 \quad \forall \boldsymbol{w}^h \in V^h_u$$

(2) Find $\boldsymbol{u}^h_{n+\theta} \in (S^h_u)_{n+\theta}$ and $p^h_{n+\theta} \in S^h_p$ such that

$$\int_\Omega w^h \cdot \rho(u^h_{n+\theta} - \tilde{u}^h_{n+\theta})/(\theta\, \Delta t)\, \mathrm{d}\Omega + \int_\Omega \varepsilon(w^h) : \sigma^h_{n+\theta}\, \mathrm{d}\Omega$$

$$+ \sum_{e=1}^{n_{\mathrm{el}}} \int_{\Omega_e} \epsilon^h \cdot [\rho(\boldsymbol{u}^h_{n+\theta} - \tilde{\boldsymbol{u}}^h_{n+\theta})/(\theta\, \Delta t) - \nabla \cdot \sigma^h_{n+\theta}]\, \mathrm{d}\Omega$$

$$+ \int_\Omega q^h \rho \nabla \cdot u^h_{n+\theta}\, \mathrm{d}\Omega = \int_{\Gamma_{\mathrm{h}}} \boldsymbol{w}^h \cdot \mathbf{h}^h_{n+\theta}\, \mathrm{d}\Gamma \quad \forall \boldsymbol{w}^h \in V^h_u \quad \forall q^h \in V^h_p$$

(3) Find $\tilde{\boldsymbol{u}}^h_{n+1-\theta} \in (S^h_u)_{n+1-\theta}$ such that

$$\int_\Omega w^h \cdot \rho[(\tilde{u}^h_{n+1-\theta} - u^h_{n+\theta})/((1-2\theta)\,\Delta t)]\,d\Omega$$
$$+ \int_\Omega \varepsilon(w^h) : \sigma^h_{n+\theta}\,d\Omega \quad \int_{\Gamma_h} w^h \cdot \mathbf{h}^h_{n+\theta}\,d\Gamma \quad \forall w^h \in V^h_u$$

(4) Find $u^h_{n+1-\theta} \in (S^h_u)_{n+\ldots}$ such that

$$\int_\Omega w^h \cdot \rho[(u^h_{n+1-\theta} - \tilde{u}^h_{n+1-\theta})/((1-2\theta)\,\Delta t) + u^h_{n+1-\theta} \cdot \nabla u^h_{n+1-\theta}]\,d\Omega$$
$$+ \sum_{e=1}^{n_{el}} \int_{\Omega^e} \delta^h \cdot [\rho((u^h_{n+1-\theta} - \tilde{u}^h_{n+1-\theta})/((1-2\theta)\,\Delta t)$$
$$+ u^h_{n+1-\theta} \cdot \nabla u^h_{n+1-\theta})]\,d\Omega = 0 \quad \forall w^h \in V^h_u$$

(5) Find $\tilde{u}^h_{n+1} \in (S^h_u)_{n+1}$ such that

$$\int_\Omega w^h \cdot \rho[(\tilde{u}^h_{n+1} - u^h_{n+1-\theta})/(\theta\,\Delta t) + u^h_{n+1-\theta} \cdot \nabla u^h_{n+1-\theta}]\,d\Omega$$
$$+ \sum_{e=1}^{n_{el}} \int_{\Omega^e} \delta^h \cdot [\rho((\tilde{u}^h_{n+1} - u^h_{n+1-\theta})/(\theta\,\Delta t) + u^h_{n+1-\theta} \cdot \nabla u^h_{n+1-\theta})]\,d\Omega = 0 \quad \forall w^h \in V^h_u . \tag{40}$$

(6) Find $u^h_{n+1} \in (S^h_u)_{n+\ldots}$ and $p^h_{n+1} \in S^h_p$ such that

$$\int_\Omega w^h \cdot \rho(u^h_{n+1} - \tilde{u}^h_{n+1})/(\theta\,\Delta t)\,d\Omega + \int_\Omega \varepsilon(w^h \ldots : \sigma^h_{n+1}\,d\Omega$$
$$+ \sum_{e=1}^{n_{el}} \int_{\Omega^e} \epsilon^h \cdot [\rho(u^h_{n+1} - \tilde{u}^h_{n+1})/(\theta\,\Delta t) - \nabla \cdot \sigma^h_{\ldots} \quad d\Omega$$
$$+ \int_\Omega q^h \rho \nabla \cdot u^h_{n+1}\,d\Omega = \int_{\Gamma_h} w^h \cdot \mathbf{h}^h_{n+1}\,d\Gamma \quad \forall w^h \in V^h_u \quad \forall q^h \in V^h_p .$$

REMARK 4. The parameter θ is the one used in the θ-scheme [10]; we set it to 1/3.

REMARK 5. The matrix forms corresponding to (36), (38), (39) and (40) can be solved implicitly or explicitly as described in [3]. The matrix form of the two 'Stokes sub-steps', i.e., (37) and (41), are quite similar to the matrix form of the T1 formulation; they can be solved implicitly or by treating the velocity explicitly. The results presented in this paper are based on the explicit treatment of all sub-steps. The numbers of passes used in the sub-steps are 4-2-2-2-4-2.

4. Numerical tests and observations

All computations were performed on the Minnesota Supercomputer Institute Cray X-MP (4 CPU's 16 Megawords of memory, 9.5 ns clock, and UNICOS 5.0 operating system). The codes are vectorized wherever possible. To have a better basis of comparison between the

solutions obtained by using different elements, we require that for each problem, meshes generated with different elements have the same distribution of the velocity and pressure nodes. The nodal values of the stream function and vorticity are obtained by the least-squares interpolation. For the meshes generated with the P1P1 element, these quantities are computed from the velocity field by using the meshes generated with the Q1Q1 element.

4.1. *The standing vortex problem*

This test problem was suggested to us by Gresho (see [12]). The purpose of the test is to get an indication of how much numerical dissipation a formulation introduces. The flow is inviscid and is contained in a 1×1 box. The initial condition consists of an axisymmetric velocity

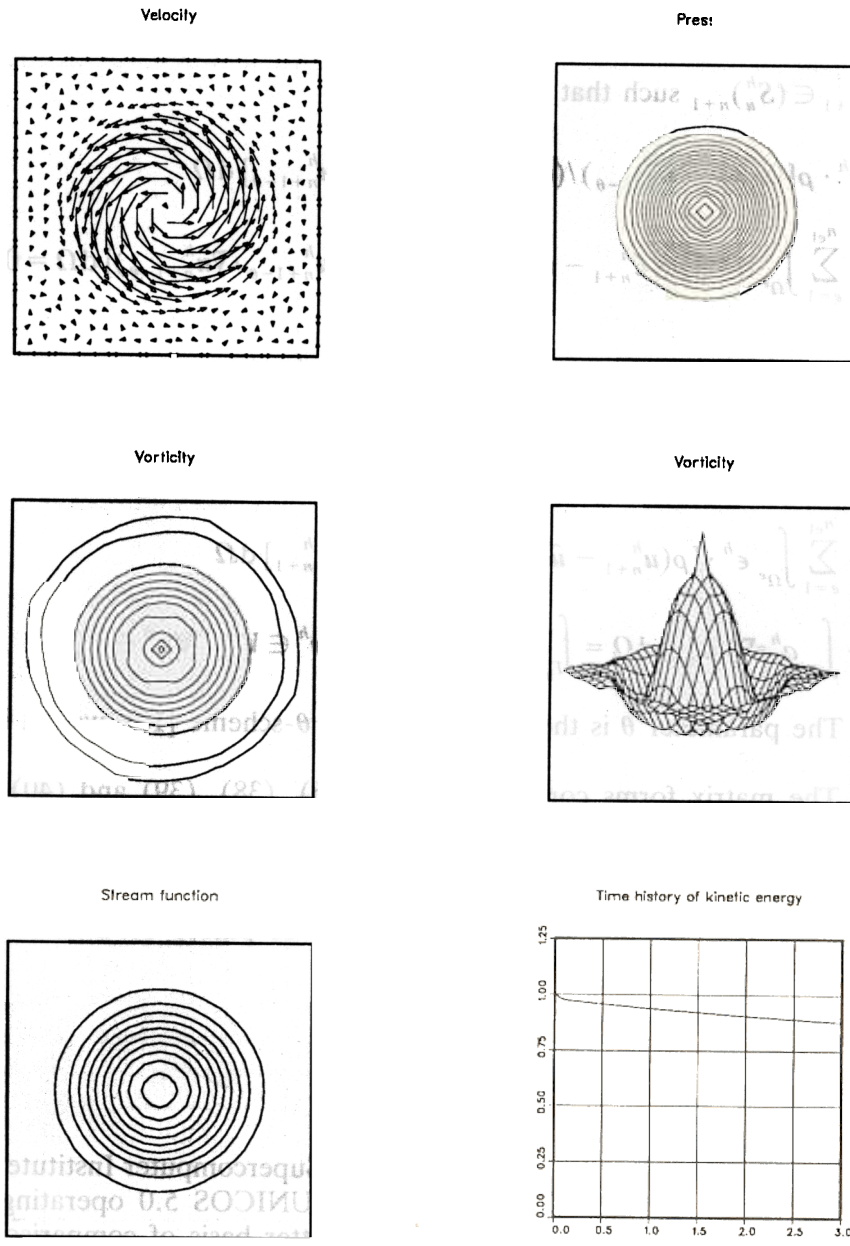

Fig. 2. Solution of the standing vortex problem at $t = 3$ with Q1Q1/T1.

profile with zero radial velocity and with the circumferential velocity given as $u_\theta = \{5r$ for $r<0.2$, $2\text{-}5r$ for $0.2<r<0.4$, 0 for $r>0.4\}$. Since this initial condition is also the exact steady-state solution, the numerical formulation should preserve this 'standing' vortex as accurately as possible. For the Q1Q1 element the finite element mesh is uniform and contains 20×20 elements. For the P1P1 element we use a mesh with 800 elements. The time step is 0.05; based on a constant 'element length' of 0.05 this results in a peak local Courant number of 1.0.

Solutions obtained at $t = 3$ (i.e. after 60 time steps) are shown in Figs. 2–5. Table 1 shows, for both elements, the percentage of the vortex kinetic energy retained after 60 time steps.

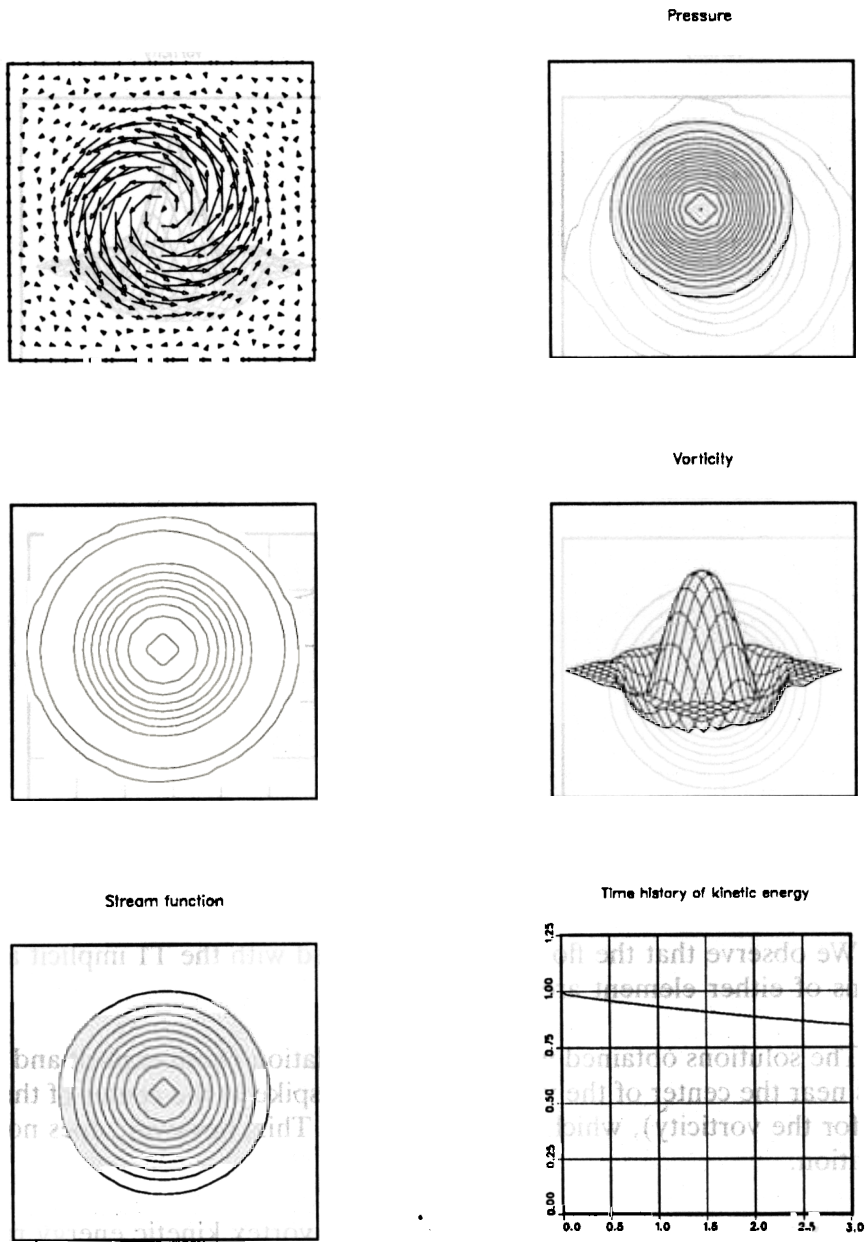

Fig. 3. Solution of the standing vortex problem at $t = 3$ with Q1Q1/T6.

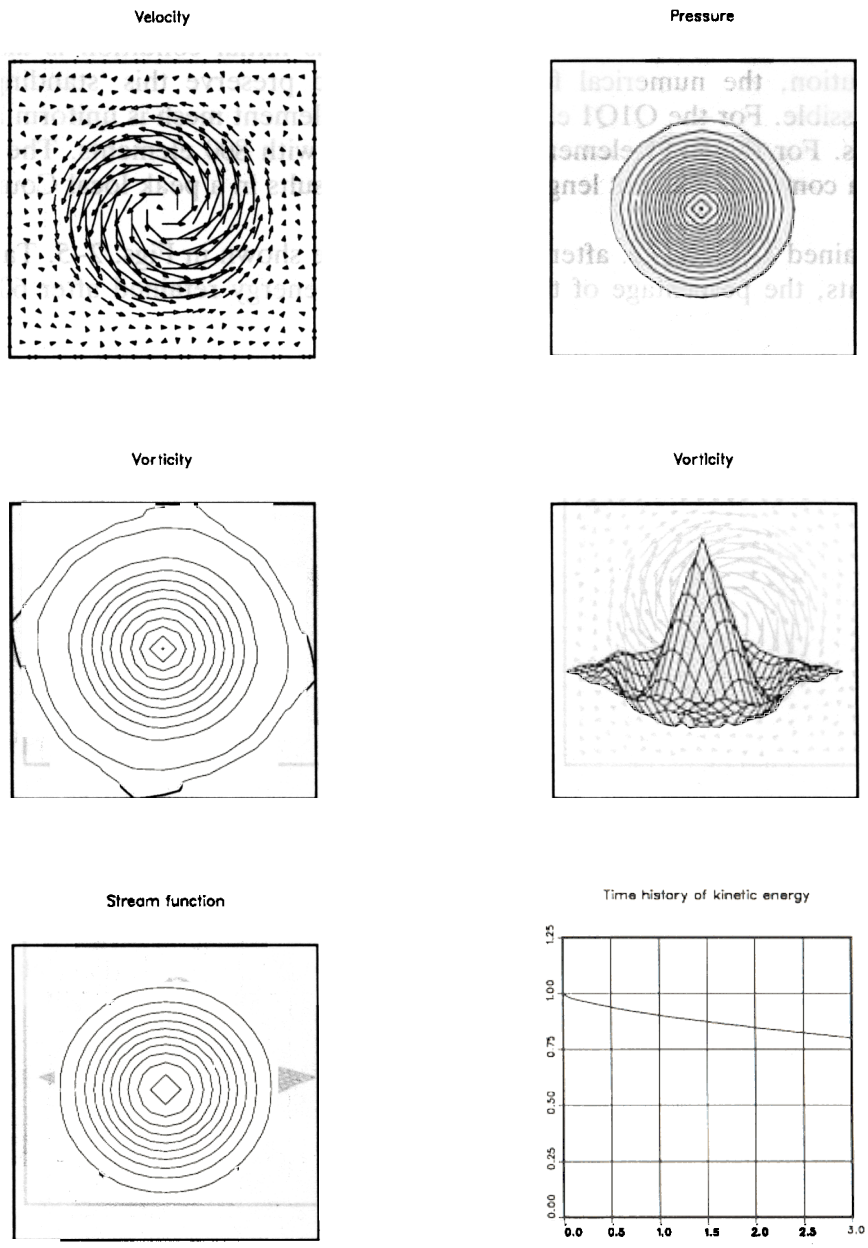

Fig. 4. Solution of the standing vortex problem at $t = 3$ with P1P1/T1

REMARK 6. We observe that the flow patterns obtained with the T1 implicit and T1 explicit implementations of either element are very similar.

REMARK 7. The solutions obtained with the T1 formulation (both explicit and implicit) have large velocities near the center of the vortex (and also a spike at the center of the vortex in the elevation plot for the vorticity), which grows with time. This, however, does not happen with the T6 formulation.

REMARK 8. When we compare the percentage of the vortex kinetic energy retained by the T6 formulation for different elements [6], we see that the Q1Q1 and P1P1 elements retain less

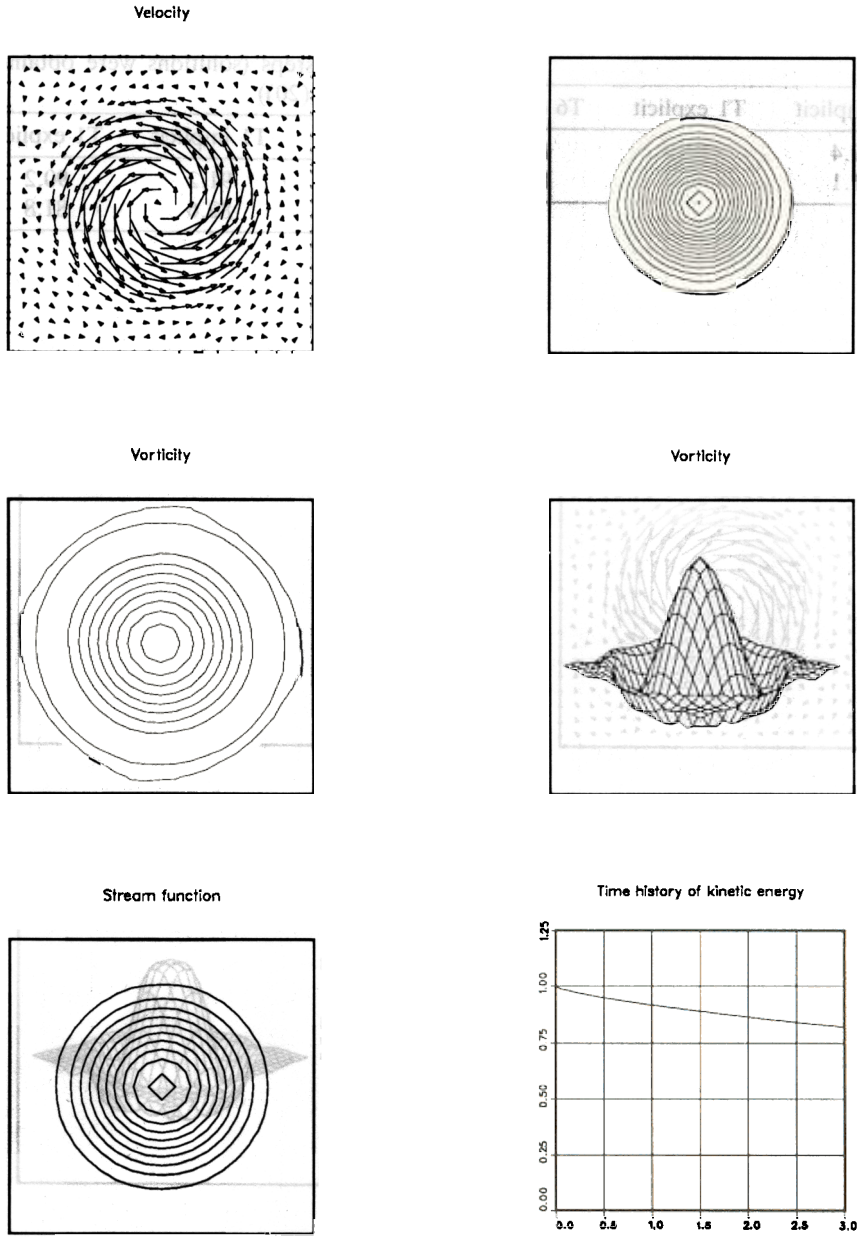

Fig. 5. Solution of the standing vortex problem at $t = 3$ with P1P1/T6.

energy than the Q1P0 (bilinear velocity/piecewise constant pressure), Q2P1 (biquadratic velocity/piecewise linear pressure) and pQ2P1 ('pseudo' quadratic version of Q2P1) elements. For the T1 formulation, on the other hand, the Q1Q1 element retains the maximum energy. The P1P1 element retains less energy than the Q2P1 and pQ2P1 elements, while the Q1P0 element has the highest energy dissipation [6].

REMARK 9. We solved the same test problem with τ_{SUPG} and τ_{PSPG} as defined by (20). The solutions obtained with the T1 formulation are shown in Figs. 6 and 7. For either element, the flow patterns obtained by using the T6 formulation are very similar to the ones obtained with

Table 1
Percentage of the vortex kinetic energy retained after 60 time steps

Element	T1 implicit	T1 explicit	T6 explicit

Table 2
Percentage of the vortex kinetic energy retained after 60 time steps (solutions were obtained with τ as defined by (20))

Element	T1 implicit	T1 explicit	T6 explicit

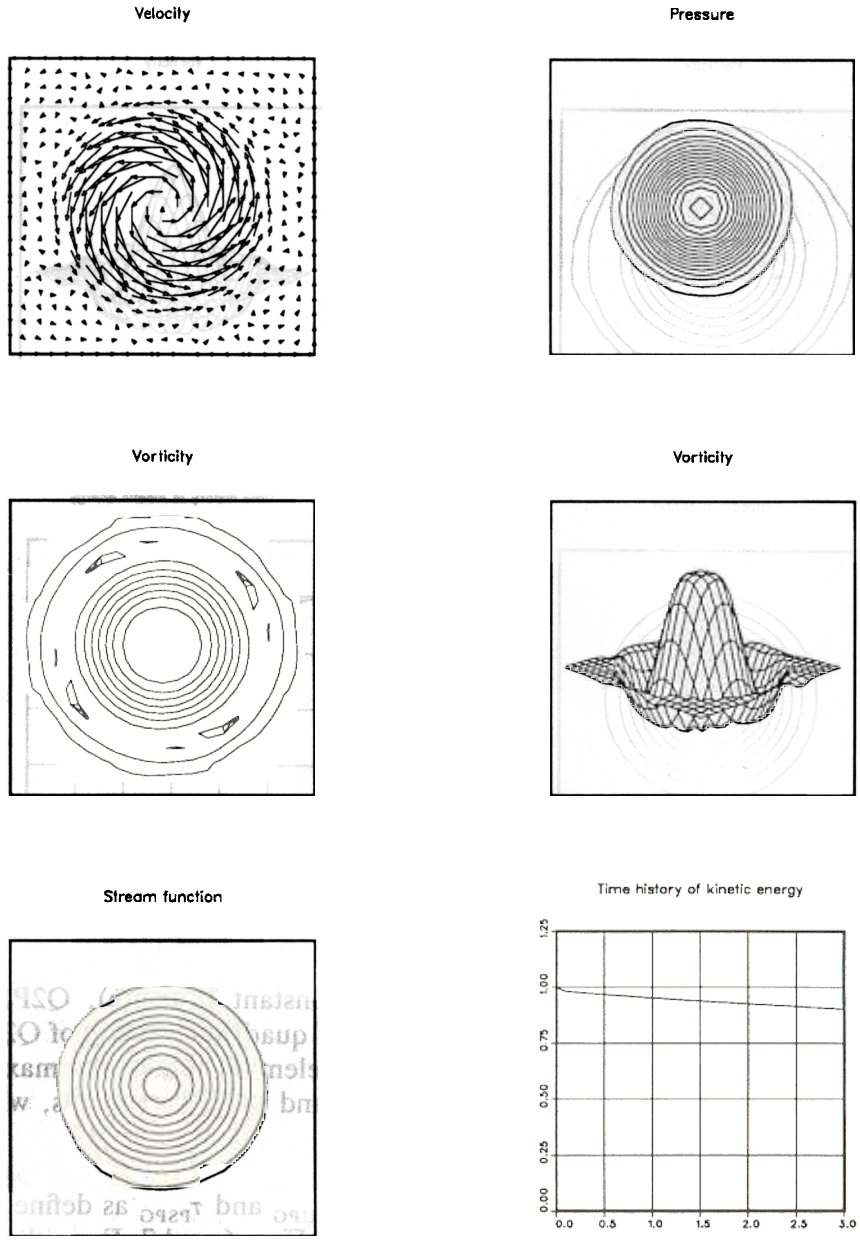

Fig. 6. Solution of the standing vortex problem at $t = 3$ with Q1Q1/T1 (with τ as defined by (20)).

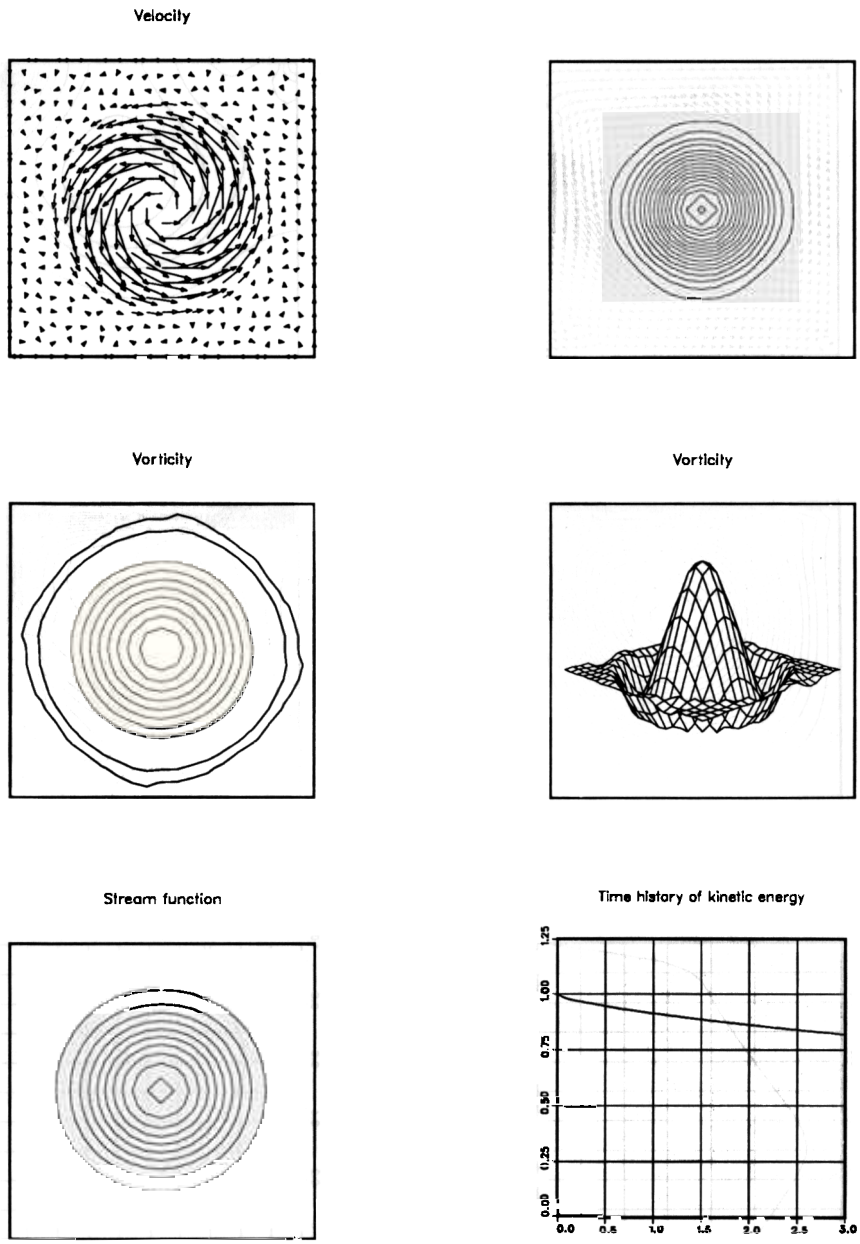

Fig. 7. Solution of the standing vortex problem at $t = 3$ with P1P1/T1 (with τ as defined by (20)).

the T1 formulation. We observe that the solutions from this formulation do not have large velocities near the center of the vortex as before (Remark 7). Table 2 shows, for both elements, the percentage of the vortex kinetic energy retained after 60 time steps.

4.2. The lid-driven cavity flow at Reynolds number 400

In this problem the lid of the cavity has unit velocity; based on this velocity and the dimensions of the cavity the Reynolds number is 400. We choose a uniform grid of 32×32 elements for the Q1Q1 element. A mesh with 2048 elements is used for the P1P1 element.

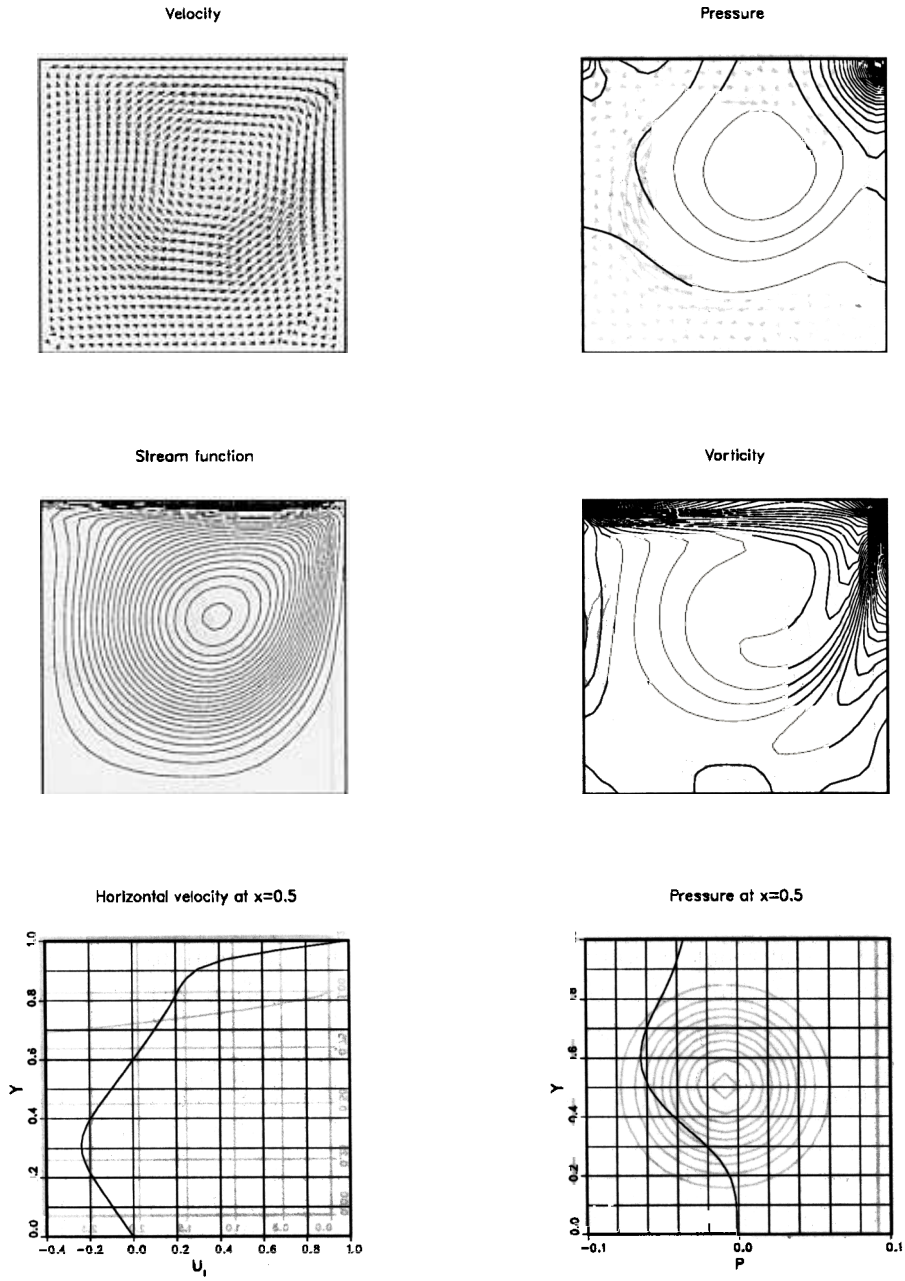

Fig. 8. Driven cavity flow at Reynolds number 400: steady-state solution obtained with Q1Q1/T1

Some of the steady-state results are shown in Figs. 8 and 9. The results obtained with the T1 and T6 implementations of both elements are all in close agreement. These results are very similar to the ones obtained with the Q1P0/T6 and pQ2P1 elements [14].

4.3. *Flow past a circular cylinder at Reynolds number 100*

In this problem we have a uniform upstream flow; the Reynolds number based on the cylinder diameter is 100. The dimensions of the computational domain, normalized by the cylinder diameter, are 30.5 and 16.0 in the flow and cross-flow directions, respectively. The

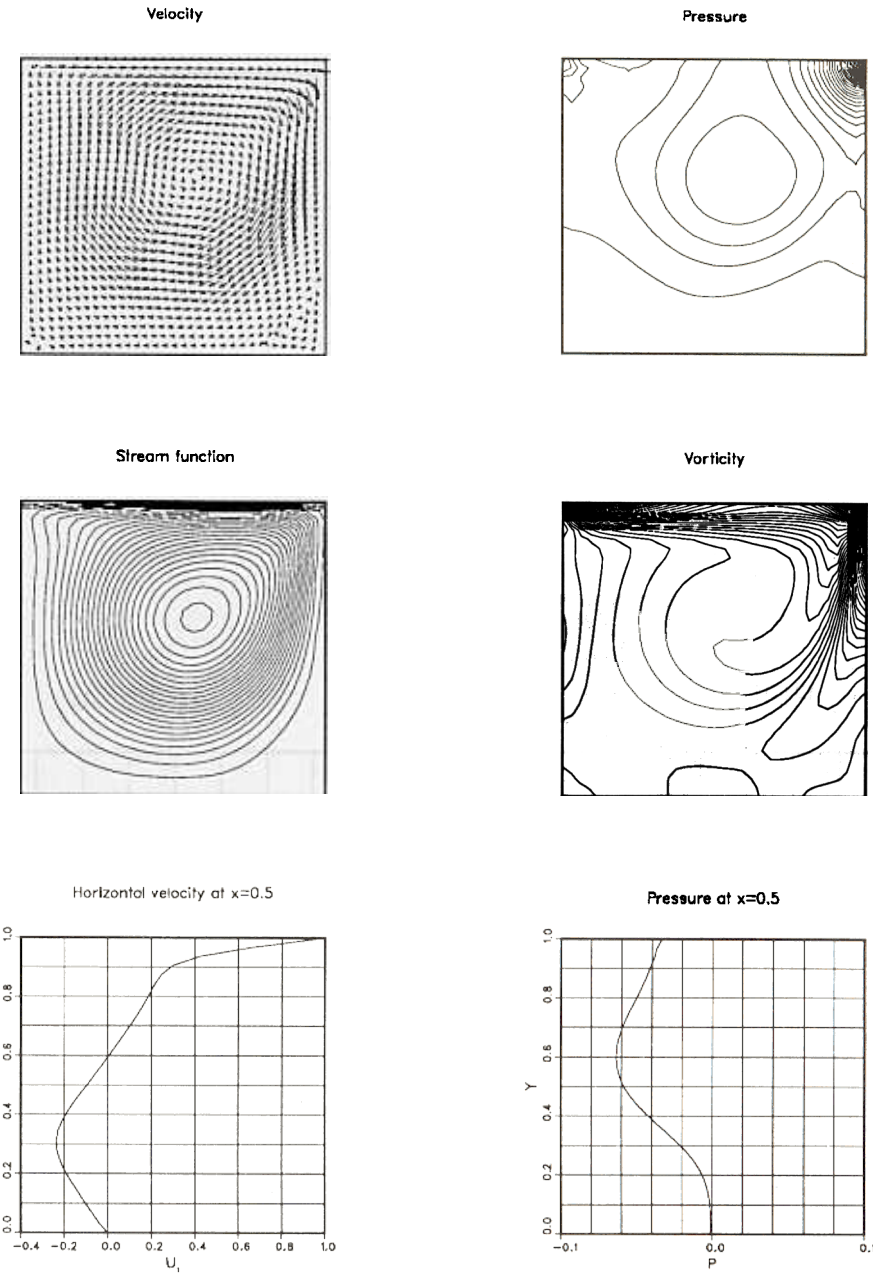

Fig. 9. Driven cavity flow at Reynolds number 400: steady-state solution obtained with P1P1/T1

mesh used for Q1Q1 consists of 5240 elements, while the number of elements for P1P1 is 10,480. Both meshes contain 5350 velocity nodes. In each case, the CPU time (in seconds) per time step is 0.76 (Q1Q1/T1), 1.69 (Q1Q1/T6), 1.07 (P1P1/T1), 1.93 (P1P1/T6). The periodic solution is computed by introducing a short term perturbation to the symmetric solution. We have observed, at least for small perturbations, that the periodic solution is independent of the mode of perturbation.

The Strouhal number and the time history of the lift and drag coefficients are shown in Figs. 10 and 11. Compared to the T1 formulation, the T6 formulation gives a slightly higher Strouhal number. Also, the Q1Q1 element gives a Strouhal number about 2% higher than the

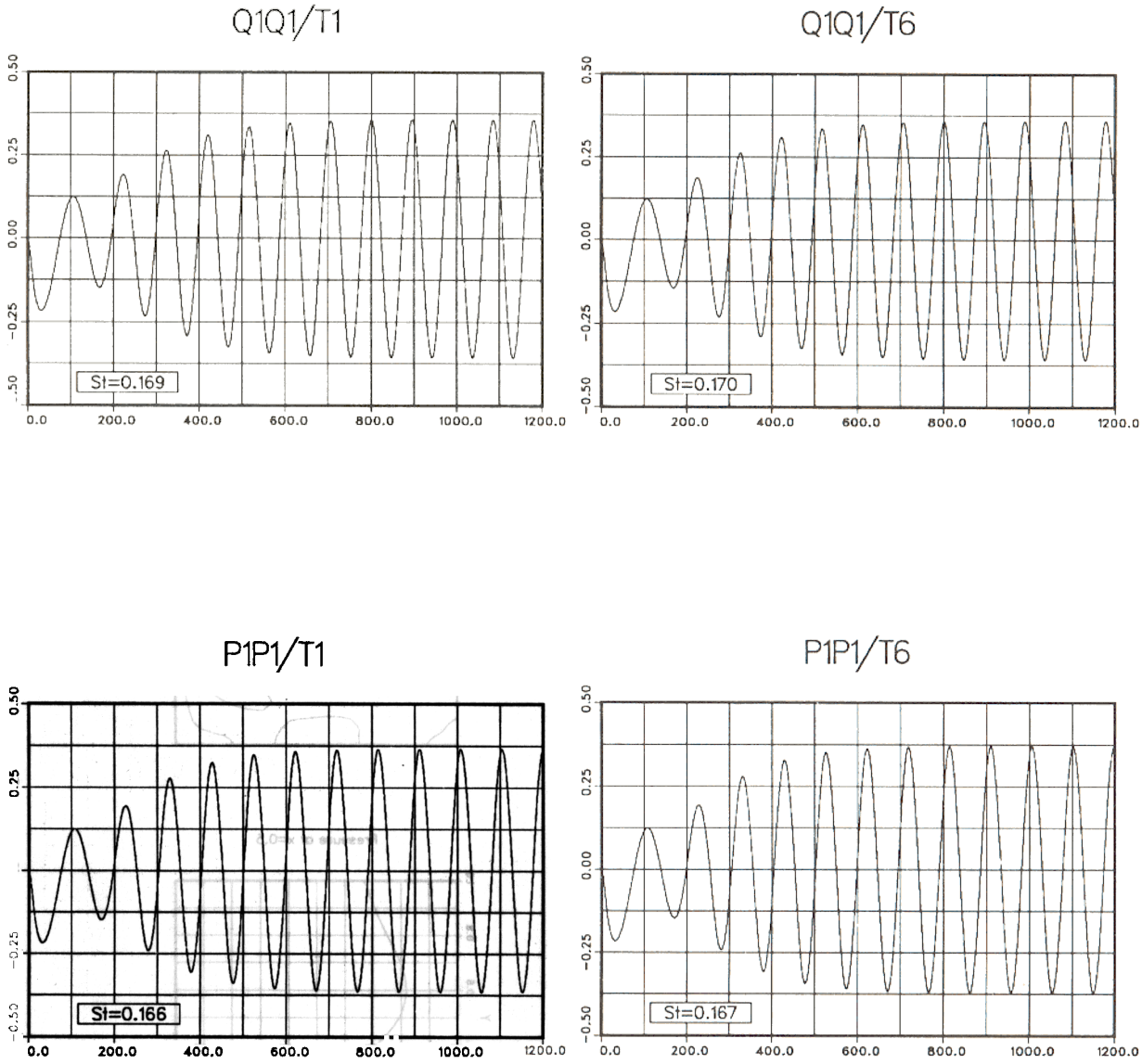

Fig. 10. Strouhal number and the time history of the lift coefficient obtained with various elements.

P1P1 element gives. Although the lift and drag coefficients show no significant difference among different formulations, the Q1Q1 element does give a slightly higher drag coefficient than the P1P1 element, and the T6 formulation gives a higher drag coefficient than the T1 formulation.

The periodic flow patterns corresponding to the crest value of the lift coefficient are shown in Figs. 12–15. The patterns corresponding to the trough value of the lift coefficient are simply the mirror images, with respect to the horizontal centerline, of the patterns shown in Figs. 12–15. We observe that the solutions obtained with different formulations are very similar. However it can be seen, upon close comparison, that the T6 formulation is less dissipative than the T1 formulation and that the Q1Q1 element is less dissipative than the P1P1 element. On comparing these solutions with the ones in [6] we observe that the solutions obtained with the Q1Q1 and P1P1 elements are very close to the ones obtained with the pQ2P1 and Q1P0/T6 elements.

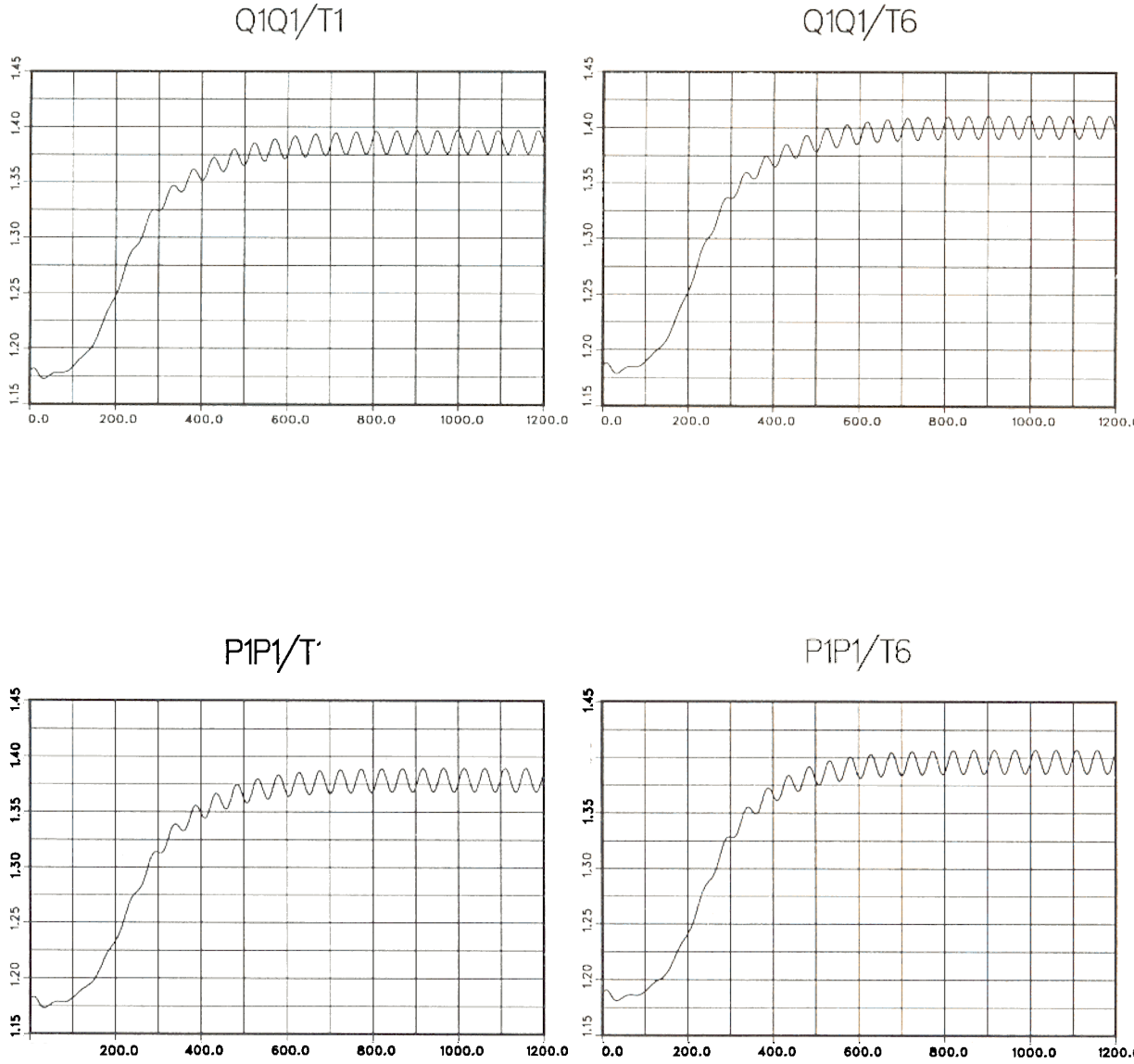

Fig. 11. Time history of the drag coefficient obtained with various elements.

We also tested on this problem, the alternative definition of τ_{SUPG} and τ_{PSPG}, as given by (20), for the implicit T1 implementation of the Q1Q1 element. We did not observe any significant difference between the steady-state solutions obtained using the two different sets of definitions for τ_{SUPG} and τ_{PSPG}.

5. Concluding remarks

We have proposed certain stabilized formulations with bilinear and linear equal-order-interpolation velocity-pressure elements for the computation of steady and unsteady incompressible flows. Equal-order-interpolation elements are very convenient from the stand-point of implementation, but need to be stabilized. The stabilization procedure involves a slightly

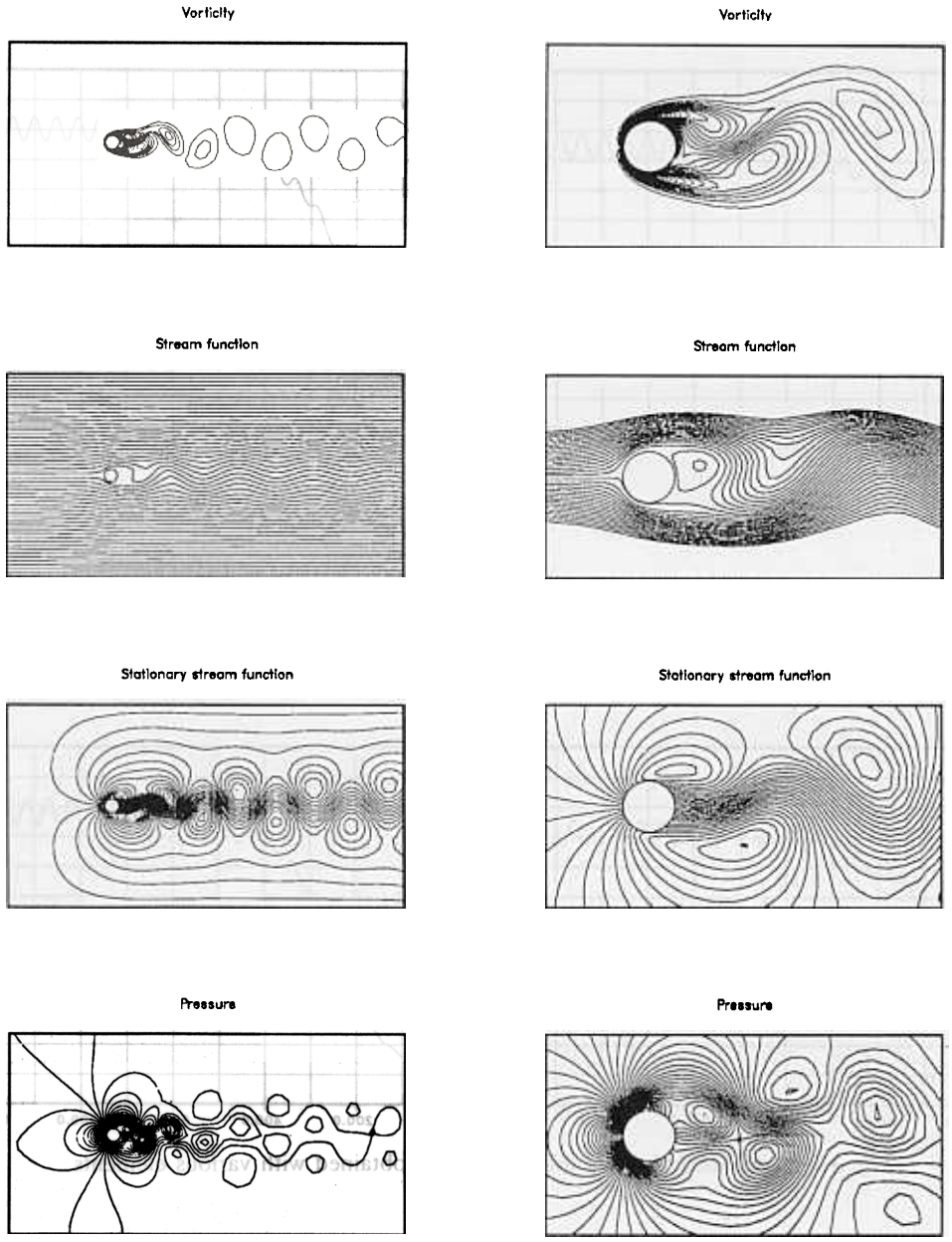

Fig. 12. Periodic solution (corresponding to the crest value of the lift coefficient) obtained with Q1Q1/T1

modified Galerkin/least-squares formulation of the steady-state equations. These elements were implemented using the one-step (T1) and multi-step (T6) formulations of the Navier–Stokes equations. We considered three numerical examples: the standing vortex problem, the lid-driven cavity flow at Reynolds number 400, and flow past a circular cylinder at Reynolds number 100. Both elements performed very well for all the test problems considered. The results from these test problems show that the Q1Q1 element is slightly less dissipative than the P1P1 element. The solutions obtained with these elements compare well with the solutions obtained with the Q1P0/T6 and pQ2P1 elements [6, 14].

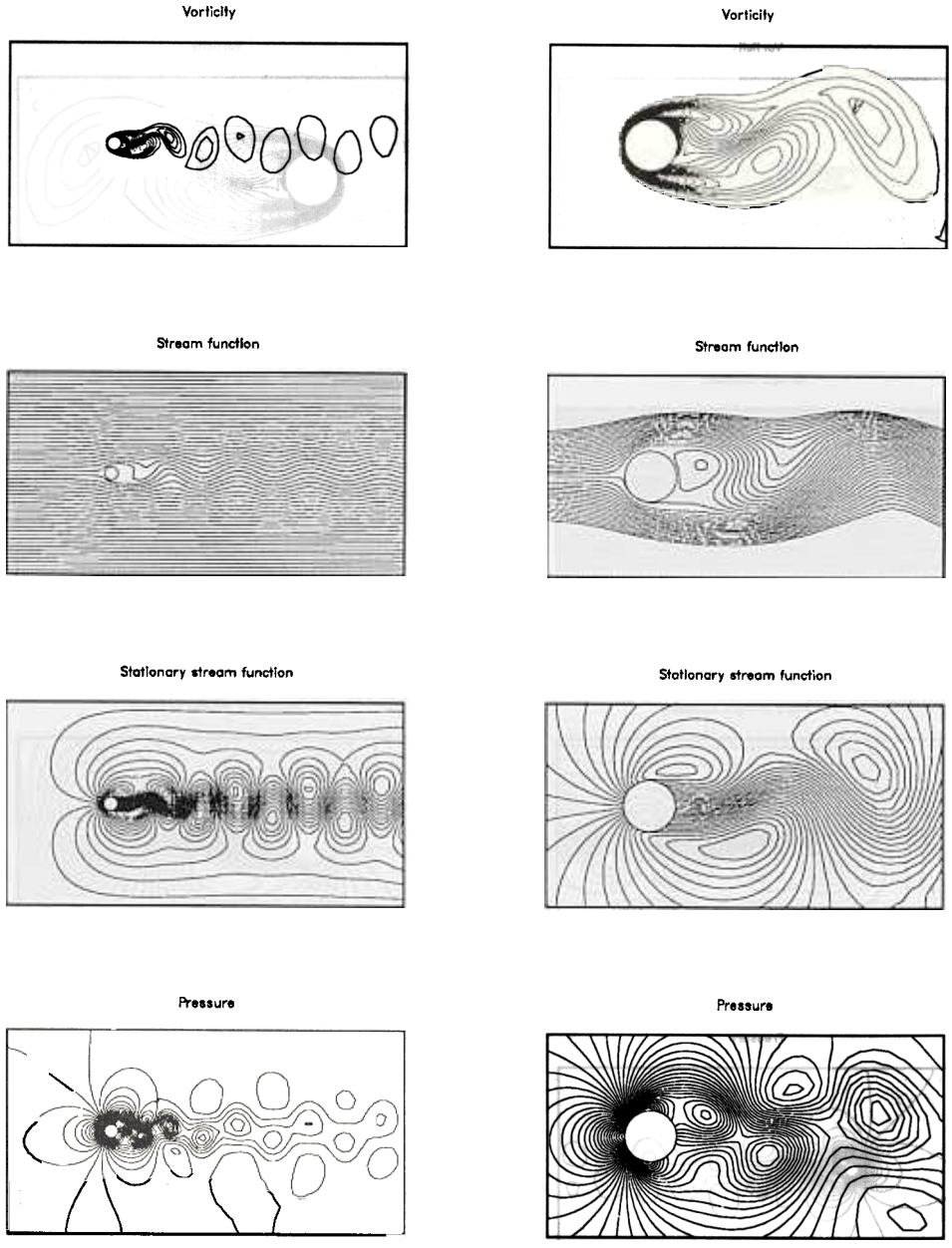

Fig. 13. Periodic solution (corresponding to the crest value of the lift coefficient) obtained with Q1Q1/T6.

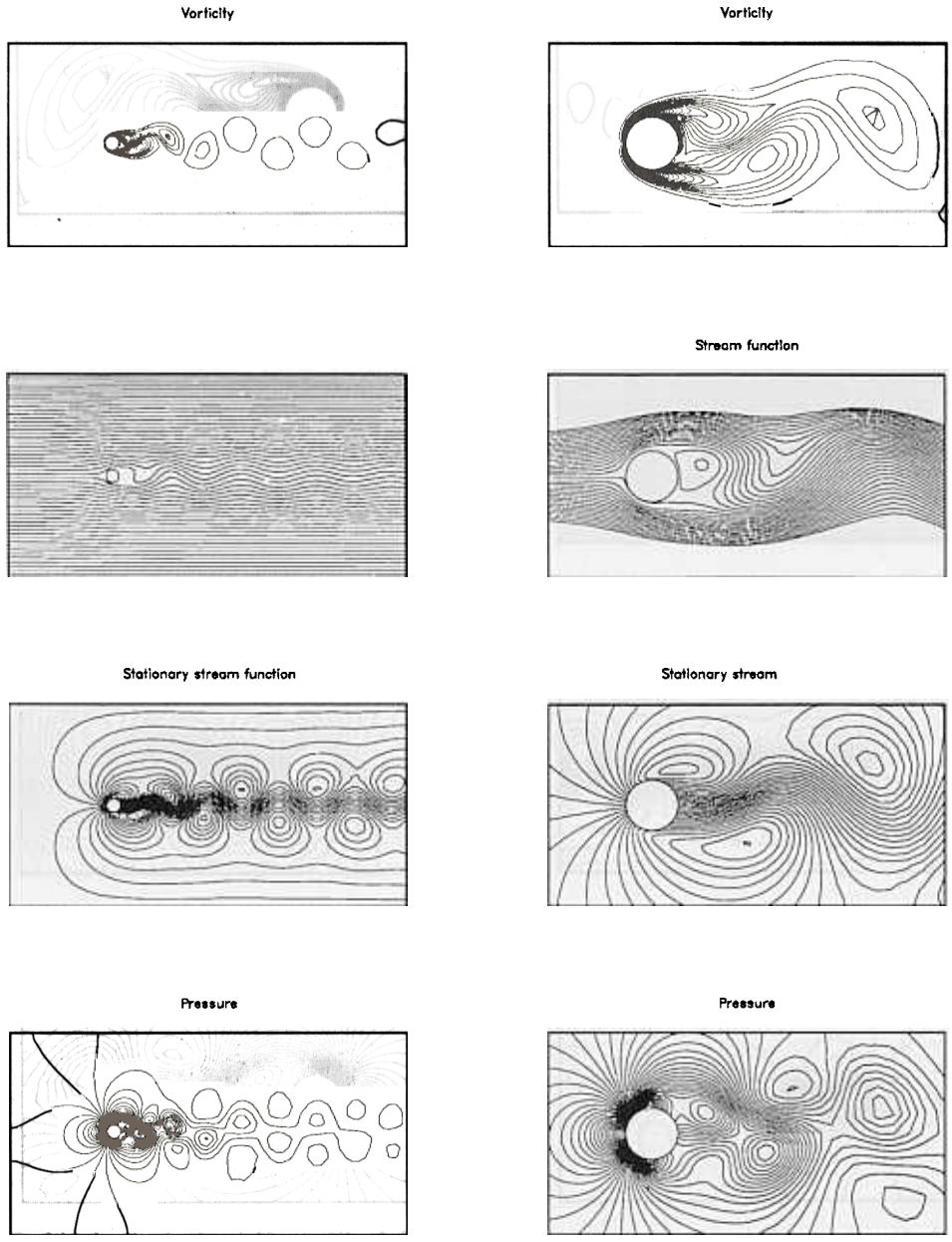

Fig. 14. Periodic solution (corresponding to the crest value of the lift coefficient) obtained with P1P1/T1

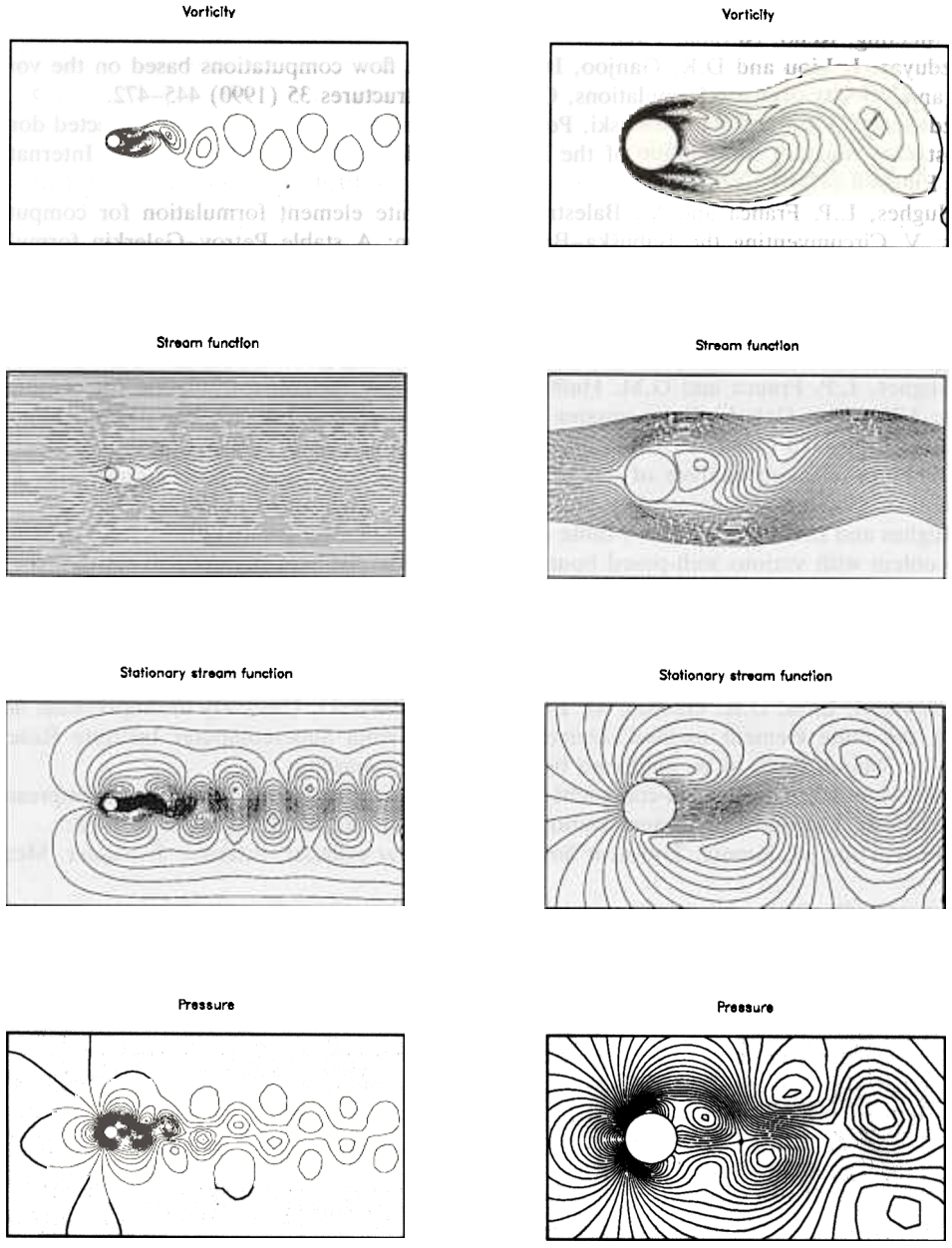

Fig. 15. Periodic solution (corresponding to the crest value of the lift coefficient) obtained with P1P1/T6.

References

[1] A.N. Brooks and T.J.R. Hughes, Streamline upwind/Petrov–Galerkin formulations for convection dominated flows with particular emphasis on the incompressible Navier–Stokes equation, Comput. Methods Appl. Mech. Engrg. 32 (1982) 199–259.

[2] T.E. Tezduyar and T.J.R. Hughes, Finite Element Formulations for convection dominated flows with particular emphasis on the compressible Euler equations, AIAA Paper 83-0125, Proc. AIAA 21st Aerospace Sciences Meeting, Reno, Nevada, 1983.

[3] T.E. Tezduyar, J. Liou and D.K. Ganjoo, Incompressible flow computations based on the vorticity-stream function and velocity-pressure formulations, Comput. & Structures 35 (1990) 445–472.

[4] T.E. Tezduyar, J. Liou and R. Glowinski, Petrov–Galerkin methods on multiply-connected domains for the vorticity-stream function formulation of the incompressible Navier–Stokes equations, Internat. J. Numer. Methods Fluids 8 (1988) 1269–1290.

[5] T.J.R. Hughes, L.P. Franca and M. Balestra, A new finite element formulation for computational fluid dynamics: V. Circumventing the Babuška–Brezzi condition: A stable Petrov–Galerkin formulation of the Stokes problem accommodating equal-order interpolations, Comput. Methods Appl. Mech. Engrg. 59 (1986) 85–99.

[6] T.E. Tezduyar, S. Mittal and R. Shih, Time-accurate incompressible flow computations with quadrilateral velocity–pressure elements, Comput. Methods Appl. Mech. Engrg. 87 (1991) 363–384.

[7] T.J.R. Hughes, L.P. Franca and G.M. Hulbert, A new finite element formulation for computational fluid dynamics: VIII. The Galerkin/least-squares method for advective-diffusive equations, Comput. Methods Appl. Mech. Engrg. 73 (1989) 173–189.

[8] F. Shakib, Finite element analysis of the compressible Euler and Navier–Stokes equations, Ph.D. Thesis, Department of Mechanical Engineering, Stanford University, Stanford, California, 1988.

[9] T.J.R. Hughes and L.P. Franca, A new finite element formulation for computational fluid dynamics: VII. The Stokes problem with various well-posed boundary conditions: Symmetric formulations that converge for all velocity/pressure spaces, Comput. Methods Appl. Mech. Engrg. 65 (1987) 85–96.

[10] M.O. Bristeau, R. Glowinski and J. Periaux, Numerical methods for the Navier Stokes equations: Applications to the simulation of compressible and incompressible viscous flows, Comput. Phys. Rep. 6 (1987) 73–187.

[11] T.E. Tezduyar, J. Liou, D.K. Ganjoo, M. Behr and R. Glowinski, Unsteady incompressible flow computations with the finite element method, University of Minnesota Supercomputer Institute Research Report UMSI 90/36, March 1990, to be published by Hemisphere Publishing.

[12] P.M. Gresho and S.T. Chan, Semi-consistent mass matrix techniques for solving the incompressible Navier–Stokes equations, Lawrence Livermore National Laboratory, Preprint UCRL-99503, 1988.

[13] M.S. Engelman and M. Jamnia, Transient flow past a circular cylinder, Internat. J. Numer. Methods Fluids, to appear.

[14] T.E. Tezduyar, R. Shih and S. Mittal, Unsteady incompressible flow computations with quadrilateral elements, in: R. Glowinski and A. Lichnewsky, eds., Computing Methods in Applied Sciences and Engineering (SIAM, Philadelphia, PA, 1990) Chapter 11, 228–248.